ORIGINAL PAPER

Effect of Ethanol Post-Treatments over Sericin Scaffolds for Tissue Engineering Applications

Maria C. Arango[1] · Yuliet Montoya Osorio[2] · John Bustamante Osorno[2] · Santiago Betancourt Parra[3] · Catalina Alvarez-López[1]

Abstract

Protein-based biomaterials are excellent candidates for biomedical applications since they have similar properties to the extracellular matrix. Recently, the use of sericin (SS), a protein present in the silk cocoon, can be used as biomaterial. To improve their properties, SS biomaterials must be subject to treatments after their manufacturing. Ethanol post-treatments by immersion and solvent vapor, are used for increasing their crystallinity, mechanical and water stability. In this work, the effect of ethanol post-treatment on the properties of SS scaffolds elaborated by the lyophilization technique was evaluated. Four post-treatments were carried out on the samples: immersed in absolute ethanol for 5 min (SS/EtOH 5 min) and for 1 h (SS/EtOH 1 h); and exposition in a saturated ethanol vapor environment for 1 h (SS/VapEtOH 1 h) and for 24 h (SS/VapEtOH 24 h). The scaffolds were characterized by X-ray diffraction (XRD) and Fourier-transform infrared spectroscopy (ATR-FTIR), scanning electron microscopy (SEM), water absorption, degradation in a phosphate-buffered saline solution, sericin release from the scaffolds, and the cytotoxicity test. The ATR-FTIR results showed an increment in the relative content of β-sheet structures and an increment in the crystallinity. SEM images revealed that the post-treatment process induces changes in treated materials to present morphological changes. The treatment materials were more water-stable. The excipients of the SS scaffolds evaluated in human epithelial fibroblasts do not generate an acute cytotoxic effect. The results suggest that ethanol post-treatments induce conformational transitions and morphological changes, which should be considered for selecting the post-treatment conditions according to developing materials for wound regeneration.

Keywords Sericin · Scaffolds · Ethanol post-treatment · Cell viability

Introduction

Silk sericin (SS) is an amorphous protein, partially soluble in water [1], which is present in the silk cocoons. Recently, SS has shown to have several properties such as anticoagulant, anticarcinogenic characteristics, biocompatibility, moisture absorption, and UV resistance [2, 3]. These properties make the SS a potentially beneficial in biomedical applications [4–6], where it has shown potential for its utilization as a biomaterial in tissue engineering, regenerative medicine and as a support element in different surgical procedures [7]. Because sericin is partially soluble in water, it has both a high release rate and rapid biodegradation in humid conditions, as well as weak mechanical properties. These characteristics limit its use for the development of materials for biomedical applications [8]. Therefore, extensive research has been carried out to modify the SS structure through different physical and chemical treatments, allowing materials with better stability and performance. One of the objectives of these treatments is to increase the content of crystalline structures such as β–sheets [9, 10].

Treatments by immersion and solvent vapor with organic solvents, like ethanol, commonly are used to induce conformational changes in SS [4]. To date, ethanol treatment, under specific conditions, has been used by different authors not only induced SS conformation from random coils to β-sheet

✉ Maria C. Arango
   camilaarangosanchez63@gmail.com

1   Grupo de Investigaciones Agroindustriales, Facultad de Ingeniería Agroindustrial, Universidad Pontificia Bolivariana, Medellín, Colombia

2   Grupo de Dinámica Cardiovascular, Centro de Bioingeniería, Universidad Pontificia Bolivariana, Medellín, Colombia

3   Grupo de Investigación Sobre Nuevos Materiales, Universidad Pontificia Bolivariana, Medellín, Colombia

[9, 11, 12], but also was an effective sterilization approach to SS scaffolds [13]. Such a method can be advantageous for biomaterials for tissue engineering applications [14]. In this work, sericin is obtained from defective cocoons, an important by-product in the silk production process, which are generally used to produce low value-added products as an alternative to make better use of these by-products and generate higher income. The aims to evaluate the effect of ethanol post-treatments (immersion 5 min and 1 h, and ethanol vapor 1 h and 24 h) on SS scaffolds properties. Chemical and crystal structure by X-Ray diffraction and Fourier-transform infrared spectroscopy (FTIR ATR). Thermal properties and morphological changes by ethanol post-treatments were studied by thermogravimetric analysis (TGA) and scanning electron microscopy (SEM), respectively. In addition, the water absorption capacity and degradation in a phosphate buffered saline solution (PBS), were evaluated in different times. The sericin release from scaffolds in PBS and cytotoxicity test were also evaluated for treated and untreated materials.

Materials and Methods

Materials

Defective cocoons (DC) were obtained from the Corporation for the Development of the Sericulture of Cauca—CORSEDA (Popayán, Colombia). DC were air dried and then hand cut in small pieces. The pupae and some impurities were removed. Commercial sericin was purchased from Aldrich (Sigma-Aldrich). The biuret reagent was acquired by the laboratory of the Bolivarian Pontifical University (Colombia) and was used for the quantification of protein in a solution. Penicillin, streptomycin, and trypsin EDTA reagents were purchased from Aldrich (Sigma-Aldrich), Dulbecco's Modified Eagle Medium (DMEM) from Lonza Bioscience and, thiazolyl blue tetrazolium bromide (MTT) from Alfa Aesar. Human epithelial fibroblasts isolated from skin biopsy samples of healthy human subjects in surgical procedure at the University IPS (Colombia), under procedures approved by the Bioethics Committee of the Faculty of Medicine of the University of Antioquia were used. The fibroblast was kindly donated by the Tissue Engineering and Cell Therapy Group of the University of Antioquia.

Silk Sericin Extraction

SS was extracted using a high temperature and pressure degumming technique (120 °C during 30 min) an autoclave (Phoenix Luferco, Brazil), in a bath ratio of 1:30 (g of cocoons in pieces/mL distilled water) [7, 15]. Obtained sericin solution was filtered using a conventional laboratory vacuum pump for removing particles and impurities. A spray dehydration process was applied maintaining an inlet temperature of 160 °C, spray flow of 40 m³/h, and flow rate of 6.3 mL/min in a Mini Spray Dryer B-290 (BÜCHI Labortechnik AG, Flawil, Switzerland). Finally, the obtained sericin powder (SSP) was stored in a glass lab desiccator.

Development of Silk Sericin Scaffold

SSP was dissolved in distilled water at a concentration of 2% (w/v) using an autoclave at the same conditions mentioned above. The obtained solution was poured into plates with 2 mL wells and then frozen at − 80 °C for 24 h [16]. The samples were lyophilized for 48 h using a freeze dryer (Labconco Corporation, Kansas, USA). The obtained aerogels were then stored in a desiccator until further characterization.

Ethanol Post Treatments

Four post treatments were carried out on the sericin materials: immersion in absolute ethanol for 5 min (SS/EtOh 5 min), immersion in absolute ethanol for 1 h (SS/EtOh 1 h), exposition to absolute ethanol steam atmosphere for 1 h (SS/VapEtOH 1 h) and exposition to absolute ethanol steam atmosphere for 24 h (SS/VapEtOH 24 h) (Fig. 1) [13, 14, 17, 18]. The control (untreated SS materials) and the treated samples were storage in a glass desiccator for 24 h. SS untreated materials were used as reference.

Characterization Methods

X-Ray Diffraction

X-ray diffraction curves were obtained using a Cu source with a diffraction range was (2θ) from 5 to 50° in an X-Ray XPert Diffractometer (Malvern PANalytical, Malvern, United Kingdom).

Fourier-Transform Infrared Spectroscopy (FTIR-ATR)

The chemical structure of sericin scaffolds was analysed using FTIR tecnique with a total attenuated reflectance module (ATR), on a Nicolet 6700 Series brand spectrometer (Thermo Electron Corporation, Beverly ma, USA). A total of 64 scans were performed at a resolution of 4 cm⁻¹ and a wavelength of 4000–400 cm⁻¹. In order to study secondary structure, as was reported by other authors [19–21], a deconvolution with Gaussian curves in the amide I region (1600–1700 cm⁻¹) was evaluated using OMNIC® software. The Eq. 1 was used to calculate the percentage of individual secondary structures, where A_m and A_T correspond to the area from individual secondary structures and the area from

Fig. 1 Illustration of the post-treatments carried out for the sericin scaffolds. **a** Immersion in absolute ethanol, and **b** exposition to absolute ethanol steam

(a)

(b)

Plastic wrap

Plastic mesh

Ethanol

Top view of the materials in the system
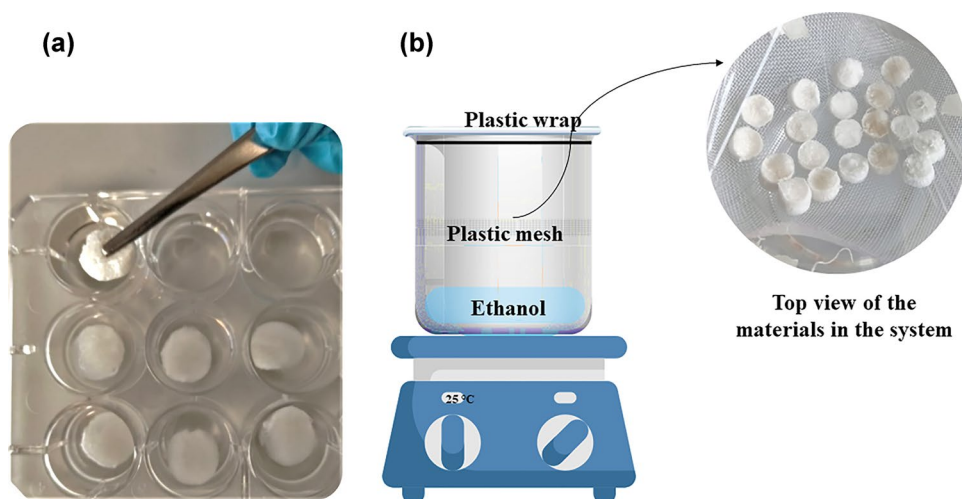
total secondary structures, respectively. The average percent was computed from three FTIR measures for each sample.

$$\text{Individual secondary structures}(\%) = \frac{A_m}{A_T} \times 100 \tag{1}$$

Crystallinity index (*CI*) was calculated by comparing the areas for absorbance intensity for β-sheets and random helices in wavelength at 1645 y 1620 cm^{-1}, respectively. The CI was obtained using the Eq. 2 [22]. The CI average was computed from three FTIR measures for each sample.

$$CI\,(\%) = \frac{A_{1620}\text{cm}^{-1}}{A_{1645}\text{cm}^{-1} + A_{1620}\text{cm}^{-1}} \times 100 \tag{2}$$

Scanning Electron Microscopy (SEM)

Secondary electrons HV-SEM technique (JSM-6490LV, JEOL, Japan) equipment was used to observe the morphology of sericin scaffolds at 5 kV. Before the observation, the samples were prepared by two cuts vertical and horizontal. Samples were covered with a thin layer of gold using a Desk IV equipment (DENTONVACUUM, Moorestown, USA), until a thickness of pprox. 10 nm was obtained.

Thermogravimetric Analysis (TGA)

The thermal behaviour of the samples was determined using a thermogravimetric analyser (TGA-Q500, Mettler Toledo, USA). In a typical experiment, 10 mg of sample were used and thermograms were obtained under an inert atmosphere of N$_2$ to avoid oxidative processes, at a rate of 50 mL/min, with a temperature range of 30–800 °C, and a uniform heating rate of 10 °C/min. With the results obtained from TGA, the first mass derivative was calculated with respect to time to obtain the degradation rate (DTG).

Water Absorption

Water absorption analysis was performed according to a modified method described by Mandal, Priya & Kundu [8]. Dry materials were weighed and then immersed in distilled water for 4, 6, 12, and 24 h. A fine mesh was used to hold the materials. The samples were extracted and, the remanent water was removed using a cotton mat before weighted. The test was replicated 3 times for each sample using the same conditions. Water absorption percent was calculated using the Eq. 3, where variables *Wh* and *Ws* are the sample weights wet and dry, respectively.

$$\%\,\text{Water absorption} = \frac{Wh - Ws}{Ws} \times 100 \tag{3}$$

PBS Degradation

The materials degradation rate was evaluated according to the method reported in [11, 12, 23]. The materials were immersed in a phosphate-buffered saline solution (PBS) with a pH value of 7.4 at 1X, in a controlled environment at a temperature of 37 °C. Weight loss was monitored at 6, 12, and 24 h. After the test, the samples were dried in a forced convection oven at 35 °C for 24 h. All experiments were carried out in triplicate. The percentage of degradation was determined according to the Eq. 4, where *Wi* is the initial weight of the dry material (before immersion) and *Wf* is the final weight of the dry sample after the immersion time.

$$\%\,\text{Degradation}\ = \frac{Wi - Wf}{Wi} \times 100 \tag{4}$$

Sericin Release from Materials

The treated and untreated materials were immersed in a 1X PBS solution (pH 7.4) in a controlled environment at a temperature of 37 °C. Subsequently, 1 mL of solution was taken from each of the samples (aliquots), after 24 h of immersion [24]. The amount of sericin released into the medium was determined by the method of Biuret [25]. Initially, a calibration curve was made using a commercial sericin standard solution with a concentration of 2% (w/v) (SIGMA brand) according to Table 1. The solutions were left to stand for 30 min at room temperature to ensure the development of colour. For reading the solutions, a UV–VIS spectrometer (Hach DR 2700, Mettler Toledo, USA) was used, the absorbance reading of the blank was given at 510 nm to adjust the absorbance baseline to 0.0. All experiments were carried out in triplicate.

In Vitro Cellular Behaviour

In Vitro Model of Human Epithelial Fibroblast Cultures Culture of epithelial fibroblast were maintained at 37 °C in DMEM medium, supplemented with fetal bovine serum (10% v/v) and penicillin–streptomycin (1% v/v). The cell cultures were incubated in flasks culture T75 under controlled conditions of 5% CO_2, 95% O_2 and, 95% relative humidity. The culture medium was changed every 3 days.

Cytotoxicity Test The metabolic reduction of 3-(4,5-dimethylthiazol-2-yl)-2,5-diphenyltetrazole (MTT) bromide was used to evaluate the effect of sericin material excipients with and without ethanol post-treatment, on the viability in human epithelial fibroblasts. MTT technique is based on the activity of the mitochondrial enzyme succinate-dehydrogenase which changes to a blue colour. This change of colour allows determining the mitochondrial functionality of cells exposed to excipients.

Epithelial fibroblasts were grown on a 96-well plate with a cell density of 3.5×10^3 cells/well. For all assay supplemented medium was used. The samples were incubated at 37 °C in a humidified atmosphere with 5% CO_2 for 48 h.

Table 1 Protein quantification by the Biuret method

	Standard protein solution (mL)	H_2O (mL)	Biuret reactive (mL)
Reference	0	1	10
1	0.25	0.75	10
2	0.5	0.5	10
3	0.75	0.25	10
4	1	0	10
Sample	1	0	10

Then, the cells were treated with the excipients from treated and untreated samples, which were obtained at periods of 4, 6, 12 and, 24 h. The cells were incubated for 24 h and then, MTT solution was added, and the formazan crystals obtained were solubilized with isopropanol. The optical density was recorded using an Elisa reader at a wavelength of 570 nm. Cytotoxicity was determined as the concentration of excipients that caused a 50% inhibition of epithelial fibroblast growth from the Eq. 5:

$$\text{Cellular viability}(\%) = \frac{\text{OD value of experimental sample (mean)}}{\text{OD value of experimental control (mean)}} \times 100 \qquad (5)$$

Statistical Analysis

To probe the differences between process conditions applied in secondary structures analysis, crystallinity index water absorption ability, weight loss, PBS degradation, and protein release, a One-way ANOVA with multiple comparisons was used (LSD Fisher test with 5% confidence level).

A minimum of three non-dependent tests were performed to evaluate the cytotoxicity. The next parameters were used: four excipients time for each scaffold type, three replicates per well, one positive control and one negative control. The statistical analysis was done with GraphPad Prism V8.0 (Intuitive Software for Science, San Diego, CA). The average values and standard deviation are presented in plots. The differences with negative control were considered with a statistically significant for *p-value* < 0.05.

Results and Discussion

The visual aspect of SS materials is presented in Fig. 2. A shrinkage was observed for materials with ethanol immersion treatment. Likewise, an increase in structural collapse for SS/EtOH 1 h sample. All samples treated with ethanol vapor preserve the shape and visual aspect of SS control material.

X-Ray Diffraction—XRD

In Fig. 3 is shown the XRD plots for evaluation samples. For the control sample (SS) is observed a broad peak near to $2\theta = 19°$ and a small shoulder to $2\theta = 22°$, which are related to crystalline space of β-sheets as has been reported in other studies [3, 12, 26, 27]. The evaluated treatments show changes in protein order as has been previously reported by other authors [28]. All samples with ethanol immersion show a high trend to increase the diffraction intensity which is associated with a reordering of the molecular structure. In fact, a slight change is observed for SS/VapEtOH
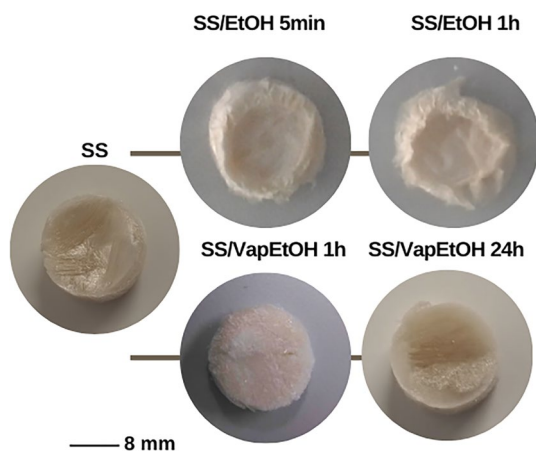
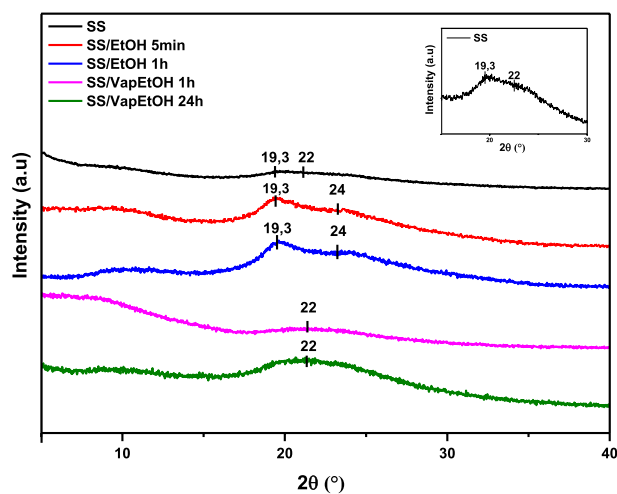**Fig. 2** Sericin scaffolds untreated and treated by immersion and ethanol vapor

Fig. 3 XRD of sericin scaffolds untreated and treated by immersion and ethanol vapor

samples which present the broad diffraction at $2\theta = 22°$ associated with sericin crystallites [29]. The curves for SS/EtOH evidence a significant change compared to SS and SS/VapEtOH. For these samples, two peaks are observed at $2\theta = 19.3°$ and $24.0°$. The first peak is related to the preservation of some original structures also reported for SS samples. The second peak can be explained as a molecular contraction of structure sericin lead a shrinkage of protein lattice parameters as a consequence of the widely recognized hydrophilic character of the protein [30]. Likewise, random structures transform to β-sheets leading to an enhancement of the order protein as has been reported [28].This finding transcends the purpose of this research and will require new studies to be carried out to explain the observed phenomenon with certainty. It is very interesting to understand this phenomenon because the molecular order of sericin plays

an important role in the chemical and physical properties of the SS materials [31, 32].

Fourier Transform Infrared—FTIR

Figure 4 shows the FTIR spectra obtained from the treated and untreated sericin materials. In Fig. 4a, four types of characteristic peaks associated with the amide groups of the protein can be observed: amide A and B (3000–3500 cm^{-1}), amide I (1600–1700 cm^{-1}), amide II (1504–1582 cm^{-1}), and amide III (1200–1300 cm^{-1}). The amide bonds form the polypeptide backbone and, due to specific vibrational frequencies, resulting in conformational changes in protein molecules [28]. Figure 4b is an enlargement of the region of amide I and II to show the changes present between the sample spectres. It was observed that the samples SS/EtOH 5 min and SS/VapEtOH 1 h show the same behaviour as the control sample, with characteristic vibrations of random spiral structures and α-helix, at wavelengths between 1652 and 1540 cm^{-1}, respectively. For SS/EtOH 1 h and SS/VapEtOH 24 h materials, the vibrations associated with random spiral structures (amide I) are located at 1622 cm^{-1}, in both samples. The amide II vibrations located at 1526 and 1525 cm^{-1}, respectively, are related to the leaf structures β-sheet and β-turns, respectively [20].

Due to the amide I is most sensitive region to variations in folding of secondary structures (22), a quantitative analysis using deconvolution models was performed. As reference point, characteristic peaks of silk sericin reported in the literature were used for the analysis. The results for almost all samples present 19 peaks that has fitted to a Gaussian curve, which are associated with different secondary structures of sericin (see Table 2) [19, 20]. Table 2 and Fig. 5 summarize the distinctive elements of secondary structures.
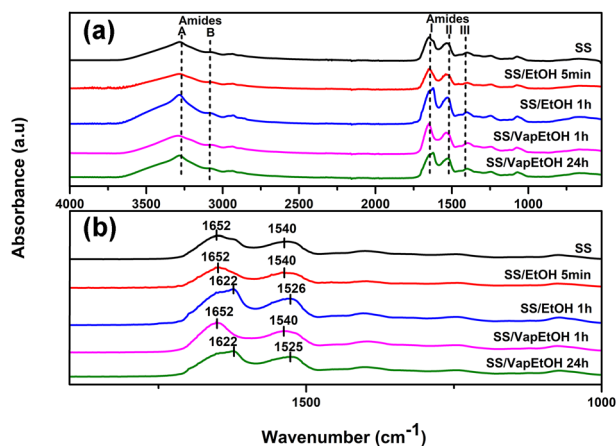

Fig. 4 FTIR spectra of untreated and treated SS materials **a** general spectrum at 400–4000 cm^{-1} and **b** zoom of spectra in amide I and amide II 1800–1000 cm^{-1}

Table 2 Percentage of secondary structures contained in the treated and untreated scaffolds

Secondary structure	Wavenumber	Percentage of crystalline structures (%)				
		SS	SS/EtOH 5 min	SS/EtOH 1 h	SS/VapEtOH 1 h	SS/VapEtOH 24 h
β-sheet	1610–1640 cm⁻¹ 1695–1700 cm⁻¹	31.46	**42.75**	**46.30**	**37.60**	**44.14**
β-turns	1660–1695 cm⁻¹	*32.30*	28.73	28.98	*32.25*	28.05
Crystalline struct		63.75	71.49	75.28	69.34	72.19
Random coil	1640–1650 cm⁻¹	14.53	11.37	**5.51**	12.72	12.9
Helix-α	1650–1660 cm⁻¹	14.19	11.25	11.91	10.48	8.79
Side chains	1600–1610 cm⁻¹	7.52	5.89	7.30	7.46	6.57
Amorphous Structures		36.25	28.51	24.72	30.66	28.26
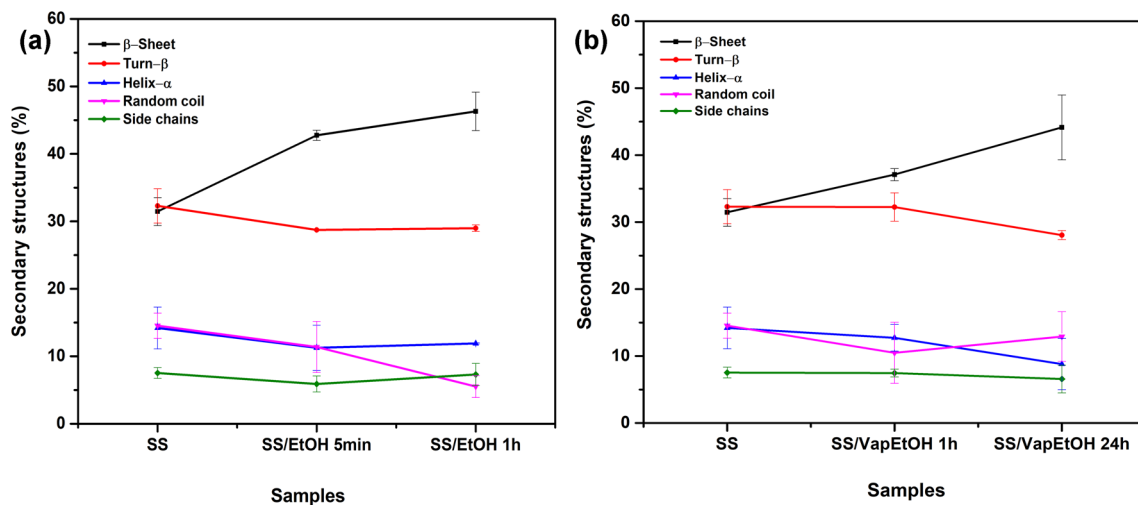
Fig. 5 Secondary structures in untreated and treated simples. **a** control and SS/EtOH materials and, **b** control and SS/VapEtOH materials. The bars represent the standard deviation (n = 3)

A statistically significant difference was found in the content of β-sheets structure for the untreated materials compared to the treated ones (*p value* < 0.05).

Treated samples show an increase in crystalline structures (β-sheets) being higher for SS/EtOH 1 h (46.3%) and SS/VapEtOH 24 h (44.41%), followed by SS/EtOH 5 min (42.75%) and SS/VapEtOH 1 h (37.6%). It has been reported that the formation of the β-sheets structures is favoured in a dehydrated state, it is because, when EtOH takes water from the molecule sericin, hydrogen bonds between sericin and water are replaced by hydrogen bonds between the sericin molecules, which induce a transition from random spirals to β-sheets [14, 22, 33].

Regarding the percentage of β-turns, SS/VapEtOH 1 h has not a difference respect to SS, while for the other samples this percentage decreases (see Table 2). On the other hand, it is evident that amorphous structures decrease in the treated samples, being more noticeable in SS/EtOH 1 h, specifically

in the random spiral structure, which went from a content of 14.53 in SS to 5.51%. This behaviour was also reported by Lamboni et al. (2015), who report a transformation mechanism where there is a decrease in random spiral structures in materials treated with ethanol, in addition to a decrease in the content of β-turns [4].

The crystallinity index is presented in Fig. 6. It was evaluated to determine the crystallinity of the samples. The results show that the untreated sample (SS) has a CI of 27.01% and an increase in the crystallinity of the materials after treatment with ethanol is observed. The highest crystallinity was presented for the SS/EtOH 1 h (61.40%) and SS/VapEtOH 24 h (50.96%) samples, followed by SS/EtOH 5 min (37.15%) and SS/VapEtOH 1 h (35.47%) samples, behaviour that coincides that observed by FTIR. According to the results obtained, SS/EtOH 5 min, SS/VapEtOH 1 h and SS samples have not a statistically significant difference between them. The SS/EtOH 1 h sample present a
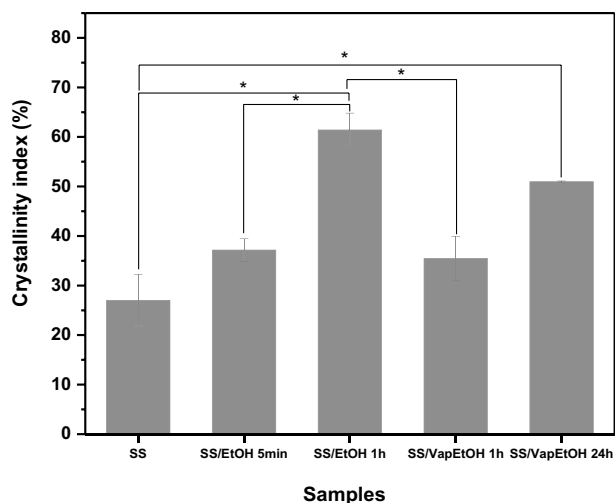
statistically significant difference with respect to all scaffolds (*p value* < 0. 05) except to the scaffold SS/VapEtOH 24 h.

The results confirm that the crystallinity of the samples increases after a longer treatment with ethanol, as evidenced by a study by Siritienthong et al. (2012), who developed SS/polyvinyl alcohol (PVA) scaffolds treated with EtOH at different concentrations (0, 60, 70, 80, 90, and 99.9 v%). Authors were looking to increase both crystallinity and structural stability of scaffolding, without the need to carry out crosslinking processes. The scaffolds obtained by this method with higher EtOH concentrations showed a higher percentage of β-sheets [17]. On the other hand, Dash et al. (2009) reported increased crystallinity in sericin membranes when treated with EtOH as found by FTIR and XRD test [28].

These results confirm that a high exposure to ethanol treatment (SS/EtOH 1 h and SS/VapEtOH 24 h) generates a

change in the crystallinity of the sample. According to Sahi, Ajay Kumar, et al. a possible mechanism of action of the treatment is the expansion of the amorphous region of the protein owing to the interruption of hydrogen bonds, which is followed by ethanol penetration in the expanded region generating a hydrophobic environment. Furthermore, the hydrophobic molecules chain segment in the random coil accumulates closely forming crystal nucleus. The growth in the crystal nucleus and rearrangement of hydrogen bonds result in a stable b-sheet conformation. Hydrogen bond rearrangement leads to water loss and creates more stable beta sheets that result in shrinkage of porous structure [34].

Sericin Material Morphology

Morphology of both untreated and treated materials was observed by SEM. Figure 7 shows that SS material has a laminar morphology with heterogeneous pores, not defined, with a honeycomb-like structure [35]. The treated materials present morphological changes, which are more evident at the SS/EtOH 1 h and SS/VapEtOH 24 h samples, where a laminar morphology, defined porosity with an average pore diameter of 70.73 and 71.01 µm, respectively, and larger apparent pore size is observed and therefore, a lower pore density compared to SS control sample. Regarding the SS/EtOH 5 min and SS/VapEtOH 1 h materials, a contraction was observed between the sheets, which showed a rougher appearance when compared whit SS/EtOH 1 h and SS/VapEtOH 24 h, presenting heterogeneous porosities like the control scaffold. The SS/VapEtOH 1 h sample has a smaller average pore diameter (69 µm) compared to the SS/EtOH 1 h and SS/VapEtOH 24 h samples (see Table 3). The importance of morphology features has impacts on physical properties such as biomechanical behaviour and water absorption capacity of the materials obtained.

The result observed in the present work can be supported by the results obtained by other authors. Siritienthong et al. (2012) observed in SS/PVA materials a thicker pore wall and
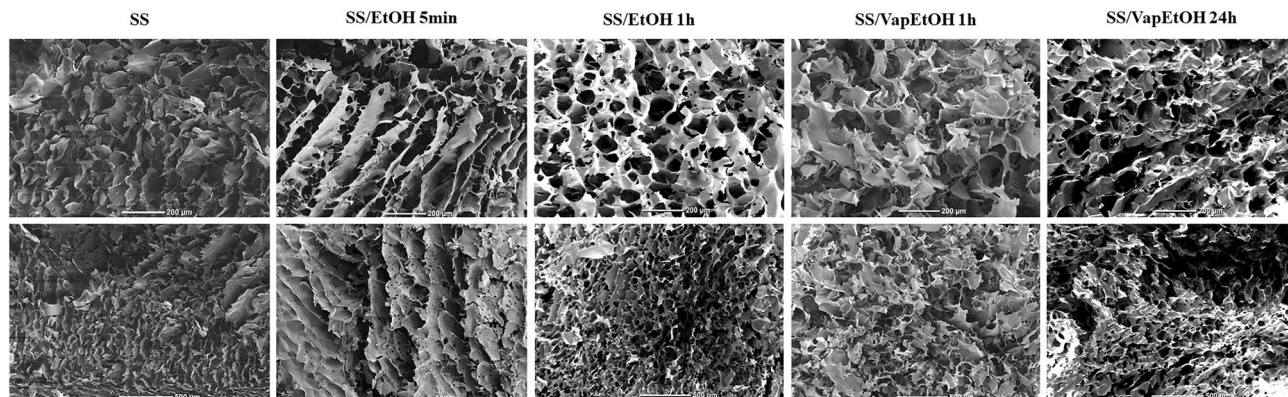

Fig. 7 Morphology of untreated and treated materials observed by SEM (200 µm and 500 µm)

Table 3 Summary of the morphological analysis and the value average pore diameter

Scaffold	Average pore diameter (μm)	Morphology
SS	Does not apply	Laminar—pores not defined
SS/EtOH 5 min	Does not apply	Laminar—contraction between the sheets
SS/EtOH 1 h	70.73	Laminar—defined porosity
SS/VapEtOH 1 h	69.00	Laminar—contraction between the sheets
SS/VapEtOH 24 h	71.01	Laminar—defined porosity

a greater roughness in the treated materials compared to the untreated ones (1). Siritientong T, Srichana T, and Aramwit P evaluated the morphology of sericin materials immersed in EtOH for 5 min in order to sterilize the material. The authors reported that the treated material exhibited reduced porosity and increased surface wrinkles [13]. It has been reported that treatment with ethanol produces a contraction in the protein material, a phenomenon explained by the hydrophobic dehydration that occurs due to molecular interactions between the protein chains and the polar solvent, which explains the differences found in the porosity of materials treated with this solvent [22].

Thermogravimetric Analysis

Figures 8a, b show the TGA and DTG curves of the untreated and treated sericin materials. The TGA curves present a thermal degradation described mainly in two stages. The first one is between 25 and 120 °C for the SS control and between 25 and 140 °C for the treated samples. This thermal event is associated to dehydration of samples by evaporation of the scaffolds remaining water. The estimated weight loss for all samples tested was near to 7%. The second stage is related to the elimination of volatile compounds and side

chains of amino acid residues degradation. From the DTG curve, two shoulders are also observed at approximately 260 and 355 °C for the SS and SS/VapEtOH 1 h samples, and at 265 and 379 °C for the other samples, in which a greater definition was achieved in the first of the peaks (Fig. 8b). Likewise, thermal event is associated with the cleavage of the peptide bonds of the protein and the carbonization of the primary structure [36–38].

Detailed results are summarized in Table 4 showing an overall similar thermal behaviour for all samples evaluated. A lower initial degradation temperature (T_{onset}) is evidenced for the SS control sample (SS) at 220 °C compared to the treated samples. The main decomposition event is assigned to the thermal degradation (T_{max}) of the protein [37]. SS and SS/VapEtOH 1 h presented a lower T_{max} (303 °C) compared to the rest of the treated samples (310 °C). This can be due to the different content of β-sheet structures between de samples as was observed in FTIR analysis. These results are related to those obtained in the crystallinity index, where a higher CI provides a higher T_{onset} and T_{max}. The results obtained have coincided with those reported for treated silk fibroin fibres with ethanol by Zuo B, Liu L, and Wu Z. The authors observed an increase in the T_{max} of the treated fibers
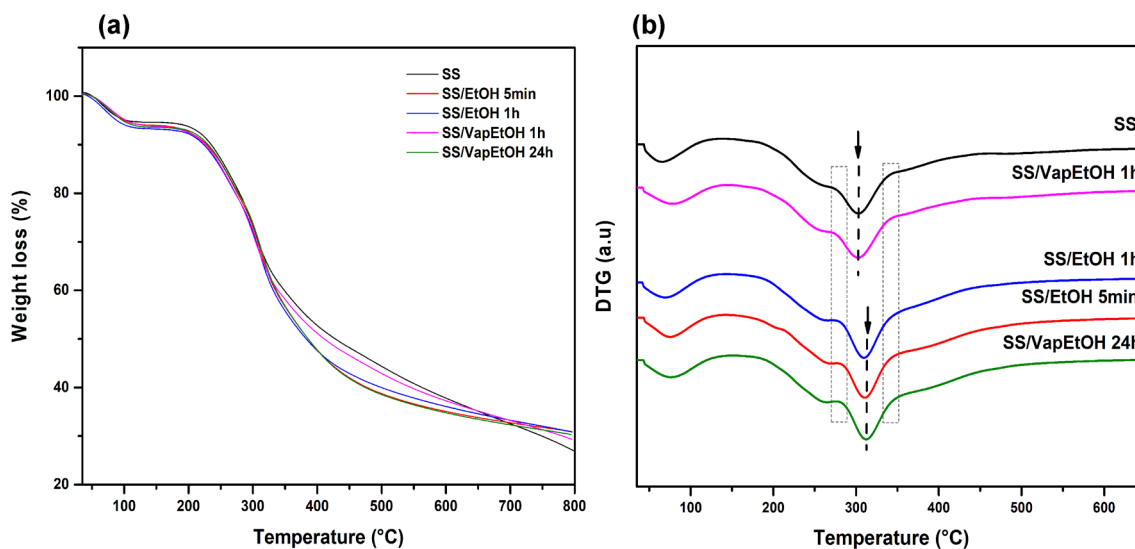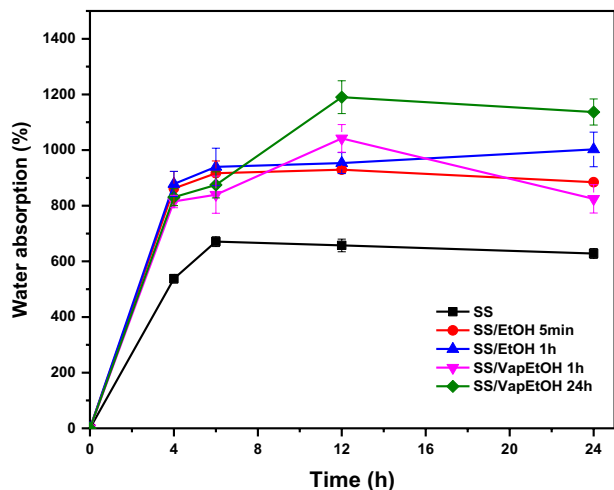

Fig. 8 **a** TGA and **b** DTG of untreated and treated materials

Table 4 T_{onset} and $T_{máx}$ of untreated and treated materials

Sample	T_{on-set} (°C)	$T_{máx}$ (°C)
SS	220	303
SS/EtOH 5 min	230	310
SS/EtOH 1 h	231	310
SS/VapEtOH 1 h	230	303
SS/VapEtOH 24 h	231	310

Fig. 9 Water absorption capacity for untreated and treated materials, exposed to different times of immersion in water. The bars represent the standard deviation (n = 3)

with respect to the untreated ones and, they describe that this behaviour because of the β-sheet structure growing [39].

Water Absorption of SS Materials

The swelling and moisture absorption capacity of SS materials are relevant characteristics for possible applications as a wound-healing dressing, which requires an absorption capacity that promotes the remotion of excess exudates while maintaining a moist condition in the wound site [40, 41]. Nevertheless, not only absorption is important, but also the stability of scaffolds during and after moisture absorption must be considered [12]. Figure 9 shows the percentage of water absorption of the treated and untreated samples after immersion in water for 4, 6, 12, and 24 h. The results show that, when the scaffolds are submerged in water, they swell rapidly in the first 4 h, reaching a 537, 862, 878, 815, and 830% increase in weight for SS, SS/EtOH 5 min, SS/EtOH 1 h, SS/VapEtOH 1 h, and SS/VapEtOH 24 h, respectively. Due to the hydrophilic nature of sericin, which is responsible for water uptake, and the large surface area of the scaffolds [8], a new weight gain is obtained in the next 2 h. This increase is greater for the control sample SS, with

133% more weight, and it was 54, 61, 24, and 44% for the SS/EtOH 5 min, SS/EtOH 1 h, SS/VapEtOH 1 h, and SS/VapEtOH 24 h scaffolds, respectively.

After 12 h, the SS scaffold shows a 13% weight loss due to the partial disintegration of the material, because of the solubility of the material and the greater amount of amorphous structures (36.25%) as evidenced in FTIR analysis. The treated samples showed an additional gain of 12 and 13% for the SS/EtOH 5 min and SS/EtOH 1 h samples, respectively. SS VapEtOH 1 h and SS/VapEtOH 24 h samples showed a greater increase compared to the scaffolds treated by immersion with 202 and 315%, respectively. After 24 h of immersion, the SS/EtOH 1 h scaffold present a new weight increase of 49%, while the SS/EtOH 5 min, SS/VapEtOH 1 h, and SS/VapEtOH 24 h scaffolds had a weight loss of 44%, 217%, and 53%, respectively. These results reveal that the SS/EtOH 1 h scaffold is the most stable sample during the immersion time. It can be explained due to the high content of hydrophobic structures β-sheet (46.3%), which avoids the disintegration of the material and gives a better water absorption ability during evaluation time. The highest weight loss of SS/VapEtOH 1 h was observed as a disintegration of the material, which may be a consequence of water saturation, to a greater amount of amorphous structures and their high-water absorption. Nevertheless, it can be concluded the ethanol treatment influences on the sericin structure and it results in more stable materials compared to the control sample.

On the other hand, the water uptake capacity of the scaffolds can be related to their morphology ("Sericin Material Morphology"). The scaffolds with denser and tighter structure (SS < SS/VapEtOH 1 h < SS/EtOH 5 min) have a smaller pore size or laminar porosity which hinders the mobility of the polymer chains and minimize their water uptake capacity. Consequently, a lower water absorption is obtained for the control sample SS, followed by SS/VapEtOH 1 h, and SS/EtOH 5 min. While for SS/EtOH 1 h and SS/VapEtOH 24 h a greater water uptake is obtained due to its major average pore diameter compared to the other samples. The results obtained in present research agree with similar results reported by Siritientong, Srichan, and Aramwit. In order to study the effectiveness of ethanol and other sterilization methods on sericin scaffolds, the authors developed SS/PVA scaffolds. The ethanol treatment was carried out by immersion for 5 min. The report indicates that the untreated and treated materials can absorb 610% of water during 24 h. As the authors claim, the untreated scaffold presented greater fragility when it was manipulated, and are disintegrated during immersion, compared to the treated scaffold, which exhibited an intact structure at the end of the treatment [42].

Sericin Release from SS Materials

Figure 10 shows the sericin release profile after 24 h of immersion of the scaffolds. A significant reduction in protein release is observed from SS materials treated with ethanol, without a statistical difference between the different treatments. The lower release of sericin from the treated materials may be related to the increase in crystalline structures and, possibly, to the new interactions that are formed
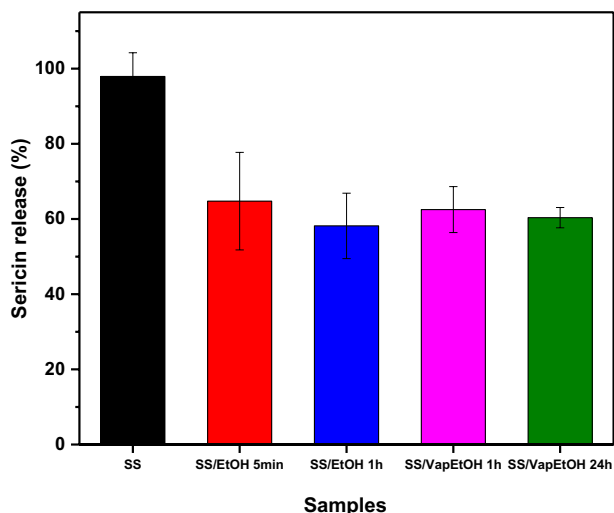
between sericin: sericin molecules, as indicated in "Fourier Transform Infrared—FTIR" (Fourier Transform Infrared—FTIR). These changes can decrease the solubility of the protein, thus improving the control of its release.

Cell Viability an In Vitro Model of Human Epithelial Fibroblasts

The percentage of cell viability was determined by the MTT test, which allows to determine the cytotoxic effect of materials in interaction with biological models in vitro. Figure 11 shows the fibroblasts viability behaviour when they are exposed to excipients from untreated and treated SS materials. The excipients obtained after 24 h from SS and SS/EtOH 5 min decrease the cell viability up to 76 and 62%, respectively, while viability SS/EtOH 1 h and SS/VapEtOH 1 h decreased up to 70%. SS/VapEtOH 24 h show the lower decreasing in cell viability (20%) after 24 h. That can be explained due to the chemical modification method favour metabolic activity and cellular integrity [43]. In addition, it is important to consider that the SS/VapEtOH 24 h material was produced for a long time, but they were not in direct contact with the solvent. This result suggests that the treated materials in ethanol immersion present changes in their microarchitecture and in their physicochemical properties, which do not favour the cell viability. In addition, direct exposure with the organic solvent may be generating free radicals and traces that are released over time and cause cell death [10].

Fig. 10 Percentage of released of untreated and treated SS materials after 24 h of immersion in PBS. The bars represent the standard deviation (n = 3)

Fig. 11 Cell viability of human epithelial fibroblasts exposed to excipients from untreated and treated SS materials, at periods of 4, 6, 12, and 24 h. The asterisk shows the statistical significance of *p < 0.05, **p < 0.01 y ***p < 0.001 compared between excipients and cells without treatment. Epithelial fibroblasts without treatment were used as a cellular control (CC)
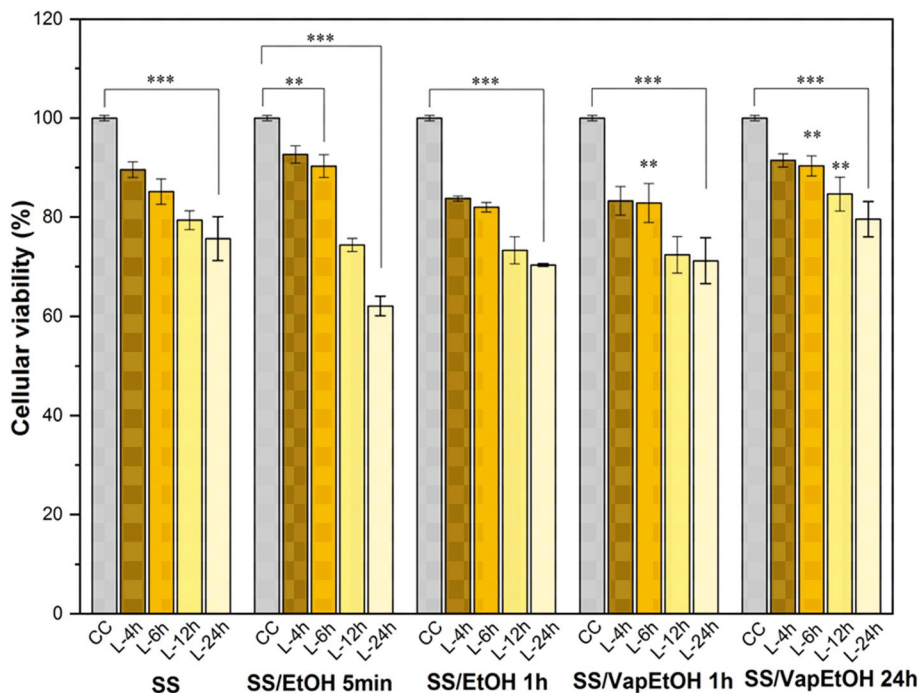
Conclusion

Regarding the ethanol immersion and steam treatments used over sericin materials, it was observed that these are effective to increase the content of secondary crystalline structures (β-sheet). This shows a structural change from the amorphous structures (random coils) to crystalline structures (β-sheets). That changes enhance thermal and water stability for all treated materials. In addition, the materials did not show disintegration during and after water absorption. All treatments increased the water absorption, which can be useful to promote the elimination of excess exudate in wounds while maintaining a wet condition in the wound place.

The excipients of the sericin from untreated and treated materials evaluated in human epithelial fibroblasts exhibit low cytotoxic effects. This behaviour is associated with a dose-concentration dependence of the release of the active compound (SS), where the greater the amount of excipient, the more cell viability is affected. Based on our results, it is proposed that sericin could be used as a bioactive compound to develop materials for wound regeneration that involve a loss of the integrity of the skin layers.

Declarations

Competing interests The authors declare no competing interests.

Competing Interest The authors have no relevant financial or non-financial interest to disclose.

References

1. Cho KY, Moon JY, Lee YW et al (2003) Preparation of self-assembled silk sericin nanoparticles. Int J Biol Macromol 32:36–42. https://doi.org/10.1016/S0141-8130(03)00023-0
2. Khan MMR, Tsukada M (2014) Silk biomaterials for tissue engineering and regenerative medicine. Elsevier, Amsterdam
3. Gupta D, Agrawal A, Rangi A (2014) Extraction and characterization of silk sericin. Indian J Fibre Text Res 39:364–372
4. Lamboni L, Gauthier M, Yang G, Wang Q (2015) Silk sericin: a versatile material for tissue engineering and drug delivery. Biotechnol Adv 33:1855–1867. https://doi.org/10.1016/j.biotechadv.2015.10.014
5. Padamwar MN, Pawar AP (2004) Silk sericin and its application: a review. J Sci Ind Res (India) 63:323–329
6. Aramwit P, Siritientong T, Srichana T (2011) Potential applications of silk sericin, a natural protein from textile industry by-products. Waste Manag Res 30:217–224. https://doi.org/10.1177/0734242X11404733
7. Chirila TV, Suzuki S, McKirdy NC (2016) Further development of silk sericin as a biomaterial: comparative investigation of the procedures for its isolation from Bombyx mori silk cocoons. Prog Biomater 5:135–145. https://doi.org/10.1007/s40204-016-0052-8
8. Mandal BB, Priya AS, Kundu SC (2009) Novel silk sericin/gelatin 3-D scaffolds and 2-D films: fabrication and characterization for potential tissue engineering applications. Acta Biomater 5:3007–3020. https://doi.org/10.1016/j.actbio.2009.03.026
9. Wang Z, Zhang Y, Zhang J et al (2015) Exploring natural silk protein sericin for regenerative medicine: an injectable, photoluminescent, cell-adhesive 3D hydrogel. Sci Rep 4:7064. https://doi.org/10.1038/srep07064
10. Neves CB, Lopes LP, Ferrão HF et al (2013) Ethanol postpolymerization treatment for improving the biocompatibility of acrylic reline resins. Biomed Res Int. https://doi.org/10.1155/2013/485246
11. Karahaliloglu Z, Kilicay E, Denkbas EB (2017) Antibacterial chitosan/silk sericin 3D porous scaffolds as a wound dressing material. Artif Cells Nanom Biotechnol. https://doi.org/10.1080/21691401.2016.1203796
12. Nayak S, Talukdar S, Kundu SC (2012) Potential of 2D crosslinked sericin membranes with improved biostability for skin tissue engineering. Cell Tissue Res 347:783–794. https://doi.org/10.1007/s00441-011-1269-4
13. Siritientong T, Srichana T, Aramwit P (2011) The effect of sterilization methods on the physical properties of silk sericin scaffolds. AAPS PharmSciTech 12:771–781. https://doi.org/10.1208/s12249-011-9641-y
14. Zhang KH, Ye Q, Yan ZY (2012) Influence of post-treatment with 75% (v/v) ethanol vapor on the properties of SF/P(LLA-CL) nanofibrous scaffolds. Int J Mol Sci 13:2036–2047. https://doi.org/10.3390/ijms13022036
15. Satya Posada Valdivia (2017) Desarrollo de esponjas de sericina a partir de hilos de seda. Universidad Pontificia Bolivariana, Medellín
16. Arango MC, Álvarez-López C (2019) Effect of freezing temperature on the properties of lyophilized silk sericin scaffold. Mater Res Express. https://doi.org/10.1088/2053-1591/ab3594
17. Siritienthong T, Ratanavaraporn J, Aramwit P (2012) Development of ethyl alcohol-precipitated silk sericin/polyvinyl alcohol scaffolds for accelerated healing of full-thickness wounds. Int J Pharm 439:175–186. https://doi.org/10.1016/j.ijpharm.2012.09.043
18. Fan L, Wang H, Zhang K, He C (2012) Regenerated silk fibroin nanofibrous matrices treated with 75% ethanol vapor for tissue-engineering applications regenerated silk fibroin nanofibrous

matrices treated with 75% ethanol vapor for tissue-engineering applications. J Biomater Sci Polym Ed. https://doi.org/10.1163/092050610X552771

19. Teramoto H, Mitsushiro M (2003) Analysis of structural properties and formation of Sericin fiber by infrared spectroscopy. J Insect Biotechnol Sericology 72:157–162

20. Adochitei A (2011) Rapid characterization of peptide secondary structure by FT-IR spectroscopy. Rev Roum Chim 56:783–791

21. Jackson M, Mantsch HH (1995) The use and misuse of FTIR spectroscopy in the determination of protein structure. Crit Rev Biochem Mol Biol 30:95–120. https://doi.org/10.3109/10409239509085140

22. Jang MJ, Um IC (2017) Effect of sericin concentration and ethanol content on gelation behavior, rheological properties, and sponge characteristics of silk sericin. Eur Polym J 93:761–774. https://doi.org/10.1016/j.eurpolymj.2017.03.048

23. Kunz RI, Brancalhão RMC, Ribeiro LDFC, Natali MRM (2016) Silkworm Sericin: properties and biomedical applications. Biomed Res Int. https://doi.org/10.1155/2016/8175701

24. Aramwit P, Siritientong T, Kanokpanont S, Srichana T (2010) Formulation and characterization of silk sericin-PVA scaffold crosslinked with genipin. Int J Biol Macromol 47:668–675. https://doi.org/10.1016/j.ijbiomac.2010.08.015

25. Colowick SP, Kaplan NO (1957) Spectrophotometric and turbidimetric methods for measuring proteins. Methods Enzymol 3:447–454

26. Thomas S (2000) Alginate dressings in surgery and wound management—part 1. J Wound Care 9:56–60. https://doi.org/10.12968/jowc.2000.9.2.26338

27. Ohnishi R, Gitoh Y, Faculty O, et al (2001) Structures and. 149–153

28. Dash BC, Mandal BB, Kundu SC (2009) Silk gland sericin protein membranes: fabrication and characterization for potential biotechnological applications. J Biotechnol 144:321–329. https://doi.org/10.1016/j.jbiotec.2009.09.019

29. Rao J, Ouyang L, Jia X, Xu Y (2011) The fabrication and characterization of 3d porous sericin/fibroin blended scaffolds. Biomed Eng: Appl Basis Commun 23:1–12. https://doi.org/10.4015/S1016237211002311

30. Ha S-W, Gracz HS, Tonelli Alan E, Hudson SM (2005) Structural study of irregular amino acid sequences in the heavy chain of bombyx mori silk fibroin. Biomacromolecules 6:2563–2569

31. Jo YN, Bae DG, Um IC (2013) The effect of extraction conditions and film side on the molecular conformation of silk sericin film. Int J Ind Entomol 26:113–118. https://doi.org/10.7852/ijie.2013.26.2.113

32. Jo YN, Um IC (2015) Effects of solvent on the solution properties, structural characteristics and properties of silk sericin. Int J Biol Macromol 78:287–295. https://doi.org/10.1016/j.ijbiomac.2015.04.004

33. Jo YN, Park BD, Um IC (2015) Effect of storage and drying temperature on the gelation behavior and structural characteristics of sericin. Int J Biol Macromol 81:936–941. https://doi.org/10.1016/j.ijbiomac.2015.09.016

34. Sahi AK, Varshney N, Poddar S et al (2021) Fabrication and characterization of silk fibroin-based nanofibrous scaffolds supplemented with gelatin for corneal tissue engineering. Cells Tissues Organs. https://doi.org/10.1159/000515946

35. Tao W, Li M, Xie R (2005) Preparation and structure of porous silk sericin materials. Macromol Mater Eng 290:188–194. https://doi.org/10.1002/mame.200400306

36. Chollakup R, Smitthipong W, Mougin K, Nardin M (2015) Characterization of sericin biomaterial from silk cocoon waste. Mater Sci Appl 1:45–50

37. Lungu A, Albu MG, Stancu IC et al (2012) Superporous collagen-sericin scaffolds. J Appl Polym Sci 127:2269–2279. https://doi.org/10.1002/app.37934

38. Rocha LKH, Favaro LIL, Rios AC et al (2017) Sericin from Bombyx mori cocoons. Part I: extraction and physicochemical-biological characterization for biopharmaceutical applications. Process Biochem 61:163–177. https://doi.org/10.1016/j.procbio.2017.06.019

39. Zuo B, Liu L, Wu Z (2007) Effect on properties of regenerated silk fibroin fiber coagulated with aqueous methanol/ethanol. J Appl Polym Sci 106:53–59. https://doi.org/10.1002/app.26653

40. Yoo M, Yong H, Lee K et al (2004) Preparation of semi-interpenetrating polymer networks composed of silk fibroin and poloxamer macromer. Int J Biol Macromol 34:263–270. https://doi.org/10.1016/j.ijbiomac.2004.06.002

41. Kamoun EA, Kenawy ERS, Chen X (2017) A review on polymeric hydrogel membranes for wound dressing applications: PVA-based hydrogel dressings. J Adv Res 8:217–233. https://doi.org/10.1016/j.jare.2017.01.005

42. Zhang D, Zhou W, Wei B et al (2015) Carboxyl-modified poly (vinyl alcohol)-crosslinked chitosan hydrogel films for potential wound dressing. Carbohydr Polym 125:189–199. https://doi.org/10.1016/j.carbpol.2015.02.034

43. Jamalzadeh L, Ghafoori H, Sariri R et al (2016) Cytotoxic effects of some common organic solvents on MCF-7, RAW-264.7 and human umbilical vein endothelial cells. Avicenna J Med Biochem. https://doi.org/10.17795/ajmb-33453